Physica B 405 (2010) 3167–3171

Contents lists available at ScienceDirect

Physica B

journal homepage: www.elsevier.com/locate/physb

# Preparation and characterization of Na-doped ZnO thin films by sol–gel method

Jianguo Lü [a,b], Kai Huang [c], Jianbo Zhu [b], Xuemei Chen [b], Xueping Song [a], Zhaoqi Sun [a,*]

[a] School of Physics and Material Science, Anhui University, Hefei 230039, China
[b] Department of Physics and Electronic Engineering, Hefei Normal University, Hefei 230061, China
[c] Department of Mathematics and Physics, Anhui University of Architecture, Hefei 230601, China

ARTICLE INFO

*Article history:*
Received 28 December 2009
Received in revised form
23 March 2010
Accepted 20 April 2010

*Keywords:*
Na-doped ZnO
Sol–gel
Atom force microscopy
Photoluminescence spectra

ABSTRACT

Undoped and Na-doped ZnO thin films were deposited on Si(1 1 1) substrate by the sol–gel method. Microstructure, surface topography and optical property of the thin films have been investigated. X-ray diffraction analysis showed that all the thin films had a polycrystalline hexagonal wurtzite structure. The 8 at% Na-doped ZnO thin films exhibited high *c*-axis preferred orientation. Surface topography revealed that average grain size of ZnO thin films annealed at 873 K increased initially, and then decreased with increasing Na concentration, and average grain size of 8 at% Na-doped ZnO thin films increased with increasing annealing temperature. PL spectra showed that all the thin films produced violet and yellow–green emissions in the visible region. In addition, the effects of Na concentration and annealing temperature on microstructure, surface topography and PL spectra are discussed.



## 1. Introduction

Zinc oxide (ZnO), with a direct band gap of 3.37 eV at room temperature and a large exciton binding energy of 60 eV, attracts considerable attention because of its promising applications for ultraviolet light-emitting diodes and laser diodes [1–5], opto-electronic devices [6–8] and surface acoustic wave devices [9–11].

So far, ZnO thin films have been prepared by means of various techniques such as magnetron sputtering [12,13], pulsed laser deposition [14,15], molecular beam epitaxy [16], sol–gel method [17] and so on. Among these techniques, the sol–gel method is popular due to its simplicity, safety and low cost. Moreover, it is easy to realize dopant incorporation and large area substrate coating. Research results showed that defects in ZnO can lead to different emission bands in the visible range. The identification of recombination centre and mechanisms responsible for many of the luminescence properties is still unclear. Various models were proposed to illustrate the emission band in ZnO [18–21].

In this paper, undoped and Na-doped ZnO thin films were prepared by the sol–gel method. X-ray diffractometry, atom force microscopy and a fluorescence spectrometer were used to investigate the influence of Na concentration on microstructure, surface topography and optical property of the thin films.

## 2. Experiments details

Ethylene glycol monomethyl ether and monoethanol amine were used as the solvent and stabilizing agent, respectively. The source for Na doping was sodium chloride (NaCl). Zinc acetate dihydrate and NaCl were first dissolved in a mixture of ethylene glycol monomethyl ether and monoethanol amine at room temperature. The concentration of zinc acetate was 0.5 mol/L. The concentration of sodium as a dopant was 0, 4, 8 and 16 at% with respect to Zn. The molar ratio of monoethanol amine to zinc acetate was kept at 1:1. The solution was stirred at 333 K for 120 min using a magnetic stirrer to get a clear, homogeneous and transparent sol, which served as the coating sol after being kept for 1 day. Na-doped ZnO thin film was deposited on Si(1 1 1) substrate using the spin coating method with 3000 rpm for 30 s. After spin coating, the substrates were kept at 423 K for 10 min to evaporate the solvent in the film and this procedure was repeated 10 times. These as-coated films were annealed for 60 min in air and then cooled down to RT.

Crystal structure of these thin films was investigated using X-ray diffractometry (XRD, MACM18XHF) with CuKα radiation ($\lambda$=0.1540 nm). Surface morphology of the thin films was measured by atom force microscopy (AFM, CSPM4000) operating in contact mode. Photoluminescence (PL) spectra were investigated at room temperature by fluorescence spectrometer (F-4500FL) with a xenon lamp as the light source excited at 325 nm.

* Corresponding author.
*E-mail address:* szq@ahu.edu.cn (Z. Sun).

0921-4526/$ - see front matter © 2010 Elsevier B.V. All rights reserved.
doi:10.1016/j.physb.2010.04.045

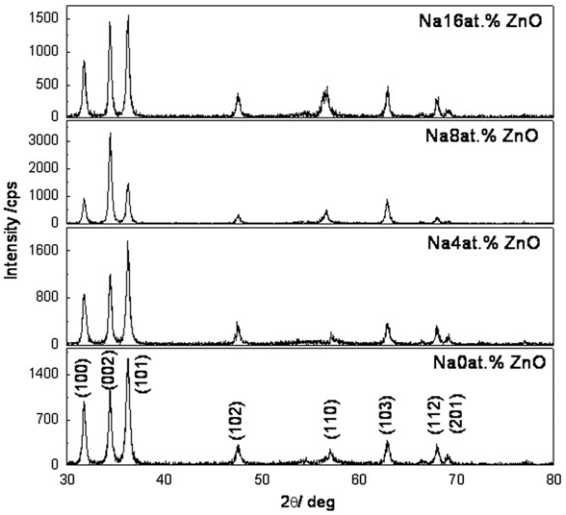


**Fig. 1.** XRD patterns of Na-doped ZnO thin films annealed at 873 K for 60 min.

## 3. Results and discussion

### 3.1. Microstructure

Fig. 1 shows XRD patterns of Na-doped ZnO thin films prepared on Si substrate with different Na concentration annealed at 873 K for 60 min. All the thin films are polycrystalline and exhibit the wurtzite structure with all XRD

**Table 1**
Variations of rms roughness of ZnO thin films.

| Thin films annealed at 873 K | | Na (8 at%)–ZnO thin films | |
|---|---|---|---|
| Na concentration (at%) | Rms roughness (nm) | Annealing temperature (K) | Rms roughness (nm) |
| 0.0 | 3.37 | 673 | 5.56 |
| 4.0 | 7.83 | 873 | 16.4 |
| 8.0 | 16.4 | 1073 | 17.9 |
| 16.0 | 16.9 | 1273 | 30.4 |

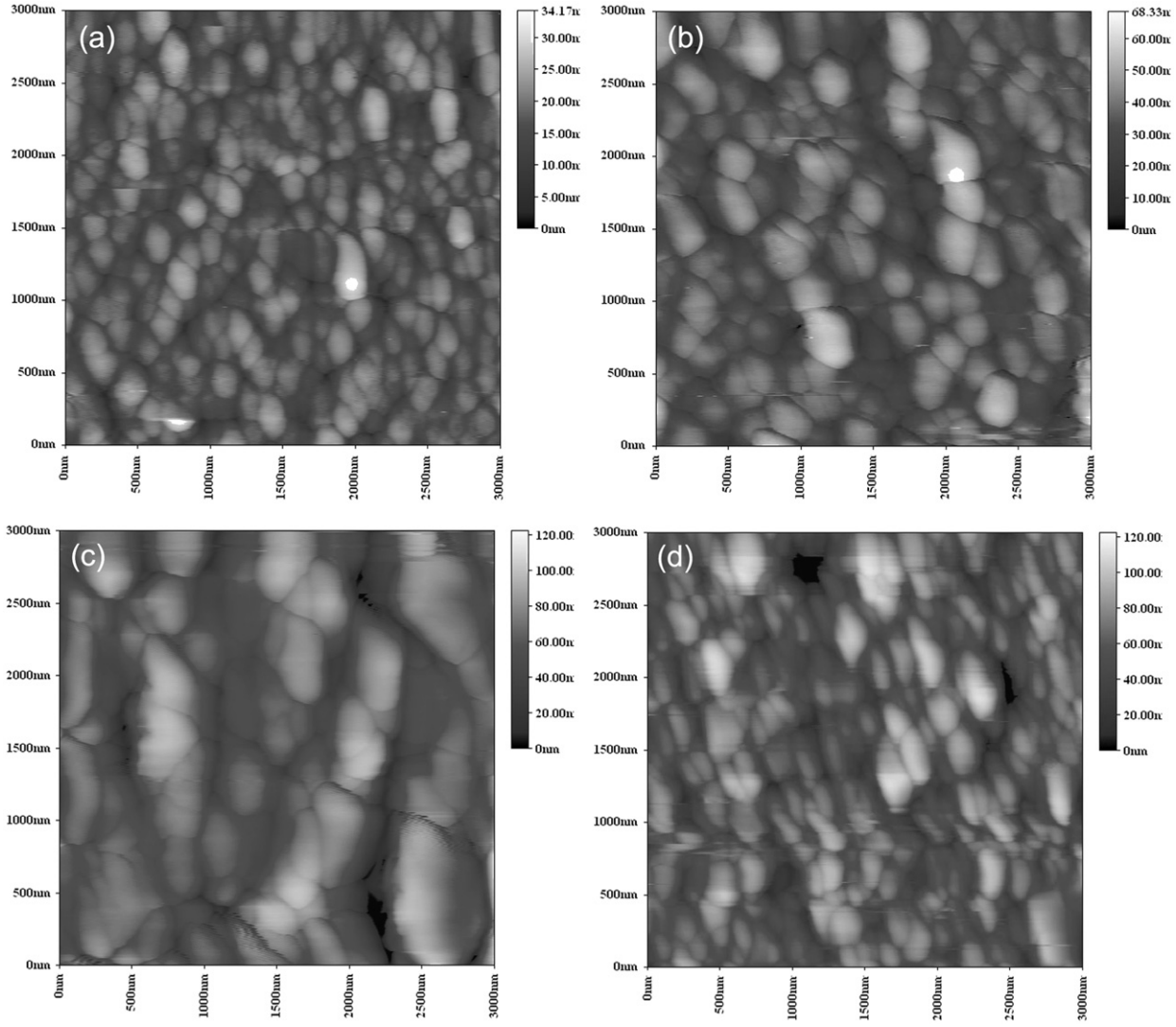


**Fig. 2.** Surface morphologies of (a) 0 at%, (b) 4 at%, (c) 8 at% and (d) 16 at% Na-doped ZnO thin films annealed at 873 K for 60 min.

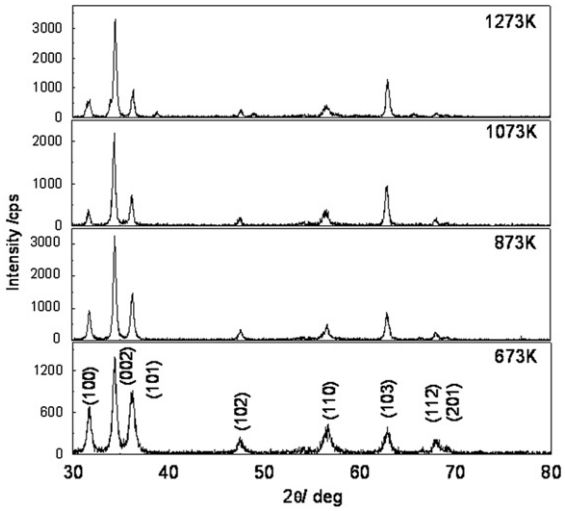


**Fig. 3.** XRD patterns of 8 at% Na-doped ZnO thin films annealed at 673, 873, 1073 and 1273 K for 60 min.

peaks identified in the recorded range. No peaks corresponding to either Na metal or any of its oxides are observed in the XRD patterns, which indicate that there is no additional phase present in Na-doped ZnO films. Added to this, Na doping almost does not affect the position of the diffraction peak, but it strongly affects the peak intensity. When the doping concentration is 8 at%, the diffraction intensity is the strongest and the intensity of (0 0 2) peak of the film is much stronger than that of other peaks, which indicates that the thin film has a better preferential *c*-axis orientation. Fig. 2 shows the surface morphology micrographs of the ZnO thin films with different Na doping concentrations. Rms roughness of the thin films are listed in Table 1. It can be seen that rms roughness of the thin films increases with increasing Na concentration. This phenomenon may be attributed to the increase of surface undulation of the thin films as Na concentration increases. However, average grain size of the thin films increase initially, and then decrease with increasing Na concentration. This result is in agreement with the X-ray diffraction patterns.

The peak intensities of the thin film increase as concentration of Na increase from 0 to 8 at%. Increasing of the peak intensities indicates that incorporation of Na greatly improves the crystallization quality of ZnO thin film, which may be because a lot of Na

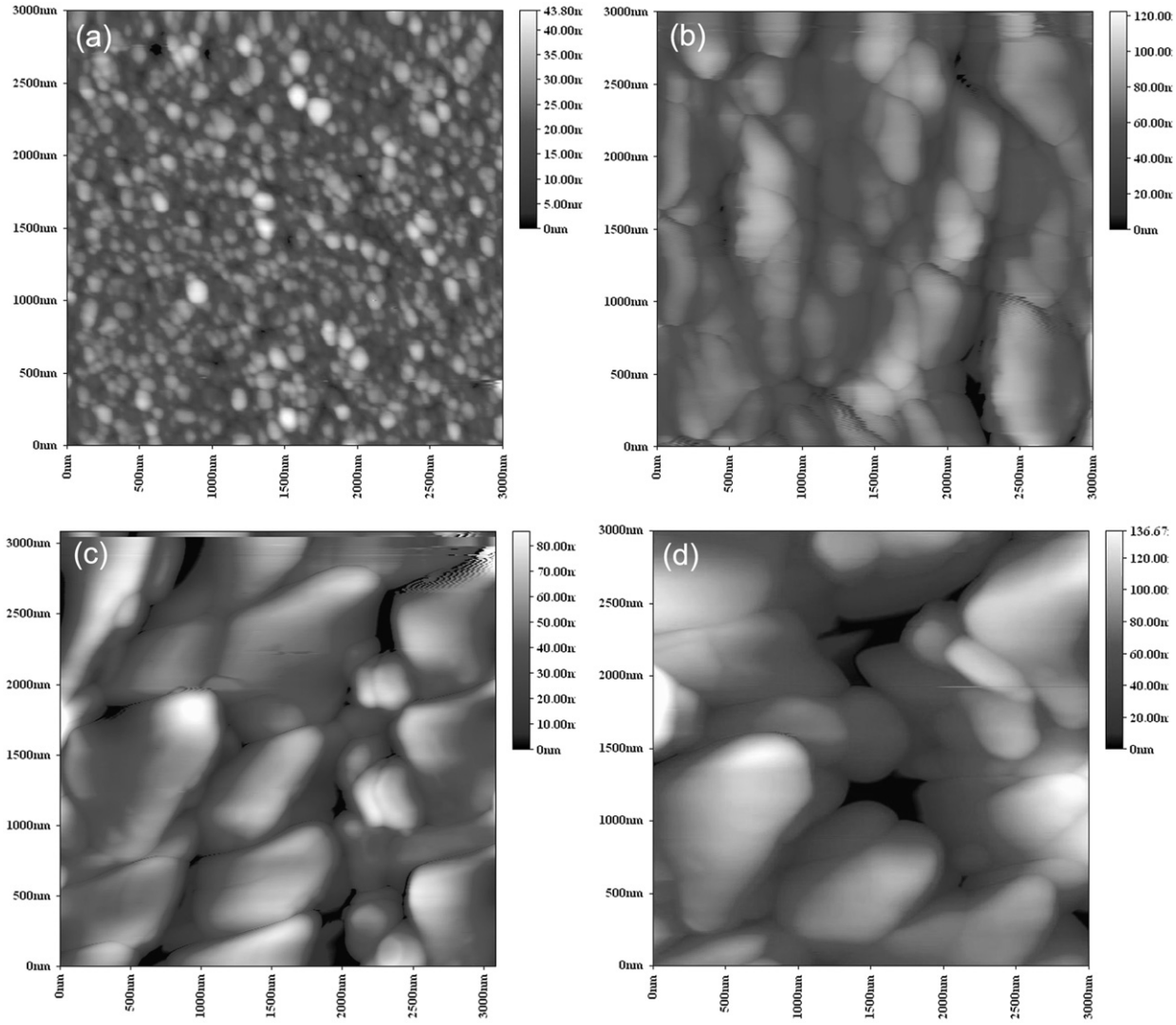


**Fig. 4.** Surface morphologies of 8 at% Na-doped ZnO thin films annealed at (a) 673 K, (b) 873 K, (c) 1073 K, and (d) 1273 K for 60 min.

ions are not substituted in the Zn sites, but as Na interstitials exist in the vicinity of the oxygen vacancies ($V_O$). They prevent lattice distortion by the $V_O$, which enhances crystallization quality [21]. However, the peak intensities of thin film decrease with further increase of Na concentration. We attribute this phenomenon to the nucleation mechanism of ZnO. As Na concentration increases, the number of nucleations of ZnO enhances and results in a smaller grain size as a consequence [22].

Fig. 3 shows the XRD patterns of Na-doped (8 at%) ZnO thin films annealed at 673, 873, 1073 and 1273 K for 60 min. The XRD patterns reveal that all the thin films are polycrystalline with hexagonal structure, and have a preferred orientation with *c*-axis perpendicular to the substrate. The intensity of the (0 0 2) peak of the thin film annealed at 1273 K has the maximum value, which indicates that the thin film has a better preferential *c*-axis orientation. Otherwise, the intensity of the (1 0 3) peak becomes more intense with increasing annealing temperature. Fig. 4 shows surface morphology micrographs of the ZnO thin films prepared on Si substrates. Rms roughness of ZnO thin films are listed in Table 1. It can be concluded that crystallization quality and average grain size of the thin film are improved with increasing annealing temperature. The increase of rms roughness of the thin film is connected with enhancement of average grain size and structural defects.

### 3.2. Optical properties

Fig. 5 shows PL spectra of the Na-doped ZnO thin films annealed at 873 K with different Na concentrations. From the spectra, it can be seen that there is violet emission in the range 380–430 nm and a yellow–green emission ranging from 450 to 600 nm. Generally, ZnO exhibits two visible bands centered at 510–540 nm (green emission) and 600–640 nm (yellow emission), attributed to oxygen vacancy ($V_O^+$) [23] and oxygen interstitial ($O_i^-$) [24], respectively. It is seen in Fig. 5 that the yellow-dominant emission for undoped ZnO thin film is switched to green emission for Na-doped ZnO thin films. The green emission peak of the samples decreases from 567 to 529 nm, and then increases to 565 nm, as Na doping concentration increases from 4 to 16 at%. This result may be connected with the competition between oxygen vacancy ($V_O^+$) and interstitial oxygen ($O_i^-$). For Na doping concentration lower than 8 at% samples, Na substitutions are more than Na interstitials in the Na-doped ZnO thin film. Considering charge equilibrium, the number of oxygen vacancy ($V_O^+$) is larger than that of interstitial oxygen ($O_i^-$). However, more oxygen interstitials may be produced since Na interstitials increase as Na doping concentration enhances from 8 to 16 at%. Change of the ratio of oxygen vacancy ($V_O^+$) to interstitial oxygen ($O_i^-$) results in a blue shift initially, and then a red shift of the green emission peak as Na doping concentration enhances from 4 to 16 at%.

Note that the violet emission in the range 380–430 nm centered at 400 nm appears in the samples, which has been observed in some research work. Wang et al. [25] prepared Al-doped zinc oxide (AZO) thin films by a dip coating method and found the films had weak violet emission in the range 400–450 nm in the 1123 K-annealed samples. But they do not explain the origin of the violet emission. Peng et al. [26] prepared Cu-doped ZnO thin films by the RF sputtering technique and found the films had violet emission. They ascribed the violet emission to the bottom of the conduction band and Zn vacancy ($V_{Zn}$) transition. Jin et al. [27] deposited ZnO thin films by pulsed laser deposition(PLD) and found the films had violet emission centered at 420 nm. They argued that the violet emission was due to a defect level in the grain boundaries of the ZnO crystals. In this paper, we consider that the violet emission is associated with both the Zn vacancy ($V_{Zn}$) and defects of the grain boundaries.

Fig. 6 gives PL spectra of the Na-doped (8 at%) ZnO thin films annealed at 673, 873, 1073 and 1273 K for 60 min. It can be seen that with increasing annealing temperature, green emission peak of the samples redshifts from 524 to 550 nm. Absolute intensities of the defect-related deep-level emission band in the visible region and the violet emission band are all increased. As annealing temperature increases, Na atoms have higher energy levels disengaged from the Zn sites to form Na interstitials and Zn vacancy ($V_{Zn}$) in the thin films. The red shift of the green emission peak is connected with increasing interstitial oxygen ($O_i^-$) and with increasing annealing temperatures, resulting in an increase of Na interstitials. The increase of intensity of emission band in

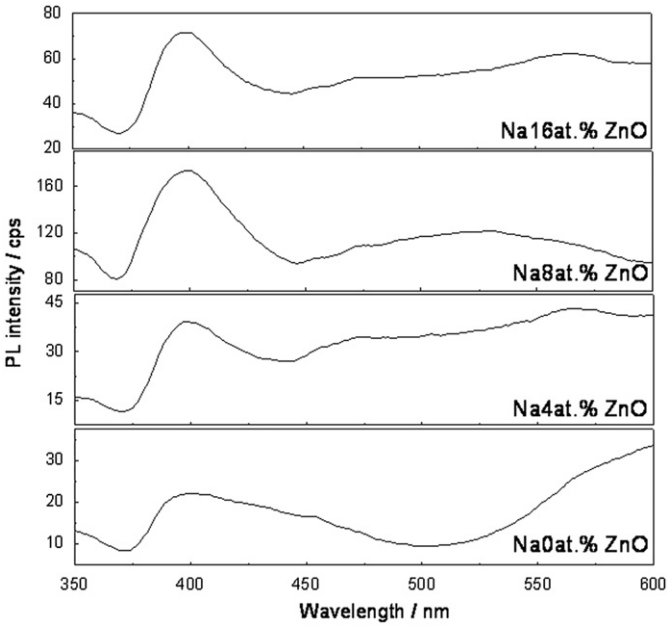


**Fig. 5.** Photoluminescence spectra of Na-doped ZnO thin films with different Na concentrations annealed at 873 K for 60 min.

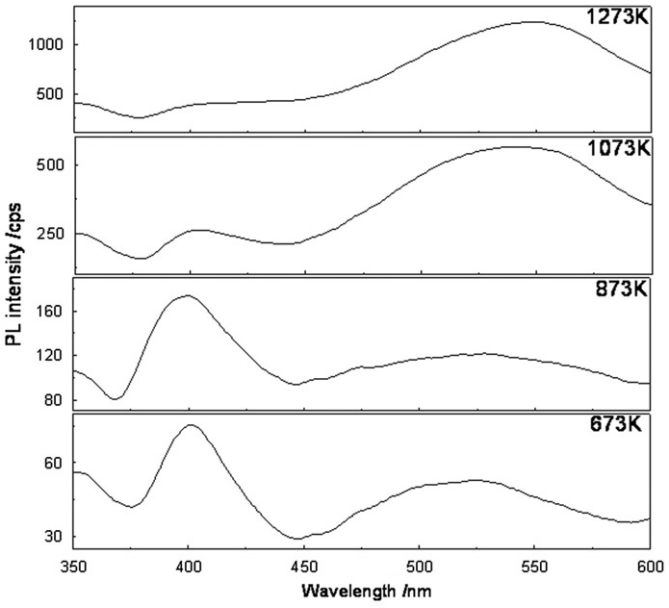


**Fig. 6.** Photoluminescence spectra of 8 at% Na-doped ZnO thin films annealed at 673, 873, 1073 and 1273 K for 60 min.

the visible region may be ascribed to structural defects. We also speculate the violet emission is associated with both Zn vacancy ($V_{Zn}$) and defect level in the grain boundaries of the ZnO crystals.

## 4. Conclusion

Na-doped ZnO films on Si (1 1 1) substrates were grown using the sol–gel process. When the doping concentration is 8 at%, intensity of the (0 0 2) peak is much stronger than that of (1 0 0) and (1 0 1) peaks. It has the maximum value for the thin film annealed at 1273 K, which indicates that the thin film has a better preferential *c*-axis orientation. As annealing temperature changes from 673 to 1273 K, rms roughness and average grain size of 8 at% Na-doped ZnO thin films increase gradually. PL spectra were investigated at room temperature. The change of green emission peak may be connected with competition between oxygen vacancy ($V_O^+$) and interstitial oxygen ($O_i^-$). The violet emission is attributed to both Zn vacancy ($V_{Zn}$) and defect level in the grain boundaries of the ZnO crystals.

## Acknowledgements

This work was supported by National Natural Science Foundation of China (no. 50872001), Research Fund for the Doctoral Program of Higher Education of China (no. 20060357003), Talent Foundation of Anhui Province (no. 2004Z029) and Natural Science Foundation of Anhui Higher Education Institution of China (no. KJ2010A284)

## References

[1] F.R. Services, Science 276 (1997) 895.
[2] D.M. Bagnall, Y.F. Chen, Z. Zhu, et al., Applied Physics Letters 70 (1997) 2230.
[3] Z.K. Tang, G.K.L. Wong, P. Yu, et al., Applied Physics Letters 72 (1998) 3270.
[4] D.C. Look, B. Claflin, Physica Status Solidi B 241 (2004) 624.
[5] S.S. Lin, J.G. Lu, Z.Z. Ye, et al., Solid State Communications 148 (2008) 25.
[6] P. Mitra, A.P. Chatterjee, H.S. Maiti, Materials Letters 35 (1998) 33.
[7] B.B. Rao, Materials Chemistry and Physics 64 (2000) 62.
[8] D.G. Baik, S.M. Cho, Thin Solid Films 354 (1999) 227.
[9] S.J. Pearton, D.P. Norton, K. Ip, W.W. Heo, The Journal of Vacuum Science and Technology B 22 (2004) 932.
[10] W.C. Shi, H.Y. Su, M.S. Wu, Thin Solid Films 517 (2009) 3378.
[11] S. Krishnamoorthy, A.A. Iliadis, Solid State Electronics 52 (2008) 1710.
[12] C. Wang, Z.G. Ji, J.H. Xi, et al., Materials Letters 60 (2006) 912.
[13] S.H. Jeong, B.N. Park, S.B. Lee, et al., Surface and Coatings Technology 193 (2005) 340.
[14] Y.Z. Zhang, J.G. Lu, Z.Z. Ye, et al., Applied Surface Science 254 (2008) 1993.
[15] X.H. Pan, Z.Z. Ye, J.S. Li, et al., Applied Surface Science 253 (2007) 5067.
[16] S.J. Jiao, Y.M. Lu, D.Z. Shen, et al., Journal of Luminescence 122–123 (2007) 368.
[17] C.Y. Tsay, H.C. Cheng, M.C. Wang, et al., Surface and Coatings Technology 202 (2007) 1323.
[18] Y.S. Kim, W.P. Tai, Applied Surface Science 253 (2007) 4911.
[19] X.H. Wang, B. Yao, D.Z. Shen, et al., Solid State Communications 141 (2007) 600.
[20] L.L. Chen, H.P. He, Z.Z. Ye, et al., Chemical Physics Letters 420 (2006) 358.
[21] S.K. Kim, S.A. Kim, C.H. Lee, et al., Applied Physics Letters 85 (2004) 419.
[22] L.H. Xu, X.Y. Li, J. Yuan, Superlattices and Microstructures 44 (2008) 276.
[23] K. Vanheusden, W.L. Warren, C.H. Seager, et al., Journal of Applied Physics 79 (1996) 7983.
[24] X.L. Wu, G.G. Siu, C.L. Fu, et al., Applied Physics Letters 78 (2001) 2285.
[25] M.S. Wang, K.E. Lee, S.H. Hahn, et al., Materials Letters 61 (2007) 1118.
[26] X.P. Peng, J.Z. Xu, H. Zang, et al., Journal of Luminescence 128 (2008) 297.
[27] B.J. Jin, S. Im, S.Y. Lee, Thin Solid Films 366 (2000) 107.